J. Fluid Mech. (1987), *vol.* 182, *pp.* 127–148
Printed in Great Britain

Effect of acoustic excitation on the flow over a low-*Re* airfoil

By K. B. M. Q. ZAMAN†, A. BAR-SEVER‡
ESCON, NASA Langley Research Center, Hampton, VA 23665, USA

AND S. M. MANGALAM
AS & M Inc., NASA Langley Research Center, Hampton, VA 23665, USA

(Received 5 November 1985 and in revised form 24 February 1987)

Wind-tunnel measurements of lift, drag and wake velocity spectra were carried out under (tonal) acoustic excitation for a smooth airfoil in the chord-Reynolds-number (Re_c) range of 4×10^4–1.4×10^5. The data are supported by smoke-wire flow-visualization pictures. Small-amplitude excitation in a wide, low-frequency range is found to eliminate laminar separation that otherwise degrades the airfoil performance at low Re_c near the design angle of attack. Excitation at high frequencies, scaling as $U_\infty^{\frac{1}{2}}$, eliminates a pre-stall, periodic shedding of large-scale vortices; U_∞ is the free-stream velocity. Significant improvement in lift is also achieved during post-stall, but with large-amplitude excitation. Wind-tunnel resonances strongly influence the results, especially in cases requiring large amplitudes. It is shown that large transverse velocity fluctuations, induced near the airfoil by specific cross-resonance modes, lead to the most effective separation control; resonances inducing only large-amplitude pressure fluctuations are demonstrated to be less effective.

1. Introduction

The present investigation is an attempt to better understand the effect of acoustic excitation on flow separation over airfoils. The benefit of 'acoustic tripping' in such flows, i.e. promoting transition and thus delaying separation, has been well known and documented by several researchers (e.g. Collins & Zelenevitz 1975; Mueller & Batill 1982; Ahuja & Burrin 1984; Maestrello 1985). By far the most extensive study, especially near stall conditions, was carried out by the group at Lockheed (see Ahuja & Burrin 1984). However, the mechanism of sound interaction has remained far from clearly understood. A host of questions could be raised that have essentially remained unanswered: (i) How does the frequency of effective excitation scale with the flow parameters? How critical is the amplitude of the incident sound wave? (ii) How does the observed effect depend on the Reynolds number, and on the angle of attack? (iii) Does the imparted sound excite the boundary layer or the separated shear layer? (iv) Available data exhibit a very strong influence of the wind-tunnel resonance on this phenomenon; exactly how does the resonance affect the results? Can wind-tunnel data still be applied in free flight or other practical situations?

The objective of the present investigation is to seek answers to these questions, especially as pertinent to low-Reynolds-number airfoils. The emphasis on low-

† Current address: NASA Lewis Research Center, Cleveland, OH 44135, USA.
‡ Currently with AS & M Inc., NASA Langley Research Center, Hampton, VA 23665, USA.

Reynolds-number operation was considered appropriate and timely in view of recent attention to such applications as high-altitude–long-endurance platforms, remotely piloted vehicles, inboard sections of helicopter rotors, etc. For a review of the problems and peculiarities arising in low-Reynolds-number airfoil operation, the reader is referred to Carmichael (1981), Mueller & Batill (1982), Lissaman (1983) and Mueller (1985). Depending on the ambient disturbances, these problems may arise for a given airfoil anywhere in the range $Re_c \lesssim 10^6$. Briefly stated, even at low angles of attack in this Re_c range, the boundary layer on the upper surface may encounter an adverse pressure gradient while still laminar, resulting in a laminar separation. The separated shear layer may then go through transition and either reattach, creating a 'separation bubble', or remain separated. In either case, the airfoil experiences a loss in the lift-to-drag ratio. It is sometimes possible to remedy the problem by the use of roughness elements to force transition, but such a method is a 'passive' one, and what may work in one flow condition may even represent a drag penalty in another.

The following, as well as previous results, underscore that acoustic excitation can not only act as an effective, 'active' method to restore airfoil performance at low Re_c but also improve stall margin at high Re_c. The present results, in addition, shed new light on the mechanisms, uncover a low-frequency organized wake flow structure prior to stall, and address each, and especially the last two, of the four questions posed earlier.

2. Facility

The experiment was carried out in an open-circuit, in-draught wind tunnel having a 1.3 m long test section with 30.5 cm × 45.7 cm rectangular cross-section. The flow entered through a 24 : 1 contraction section with a honeycomb and two screens, passed through the test section and was then exhausted by an axial fan. At $Re_c = 4 \times 10^4$, the turbulence intensity in the test section was about 0.25%, dropping to about 0.2% with increasing U_∞; the overall background sound pressure level was 87 dB (re 2×10^{-5} N/m^2), increasing with increasing U_∞. The turbulence and the sound pressure-fluctuation spectra (not shown) were free from any sharp peaks.

Figure 1 is a schematic diagram of the test section and instrumentation. The 10.2 cm chord airfoil (LRN-(1)-1007), designed and described by Mangalam & Pfenninger (1984), was mounted horizontally at mid-height; the enlarged cross-section is shown in the figure. Sound excitation was provided by means of an acoustic driver, through a 1.27 cm hole on the floor of the test section. A $\frac{1}{4}$ in. (B&K) microphone, flush mounted on the floor, was used to monitor the sound pressure level. The wake rake, consisting of twenty three total head tubes and one static head tube, provided the velocity profile and hence the profile drag of the airfoil. Lift was calculated by integration of the pressure distribution around the airfoil obtained by 22 static pressure taps at mid-span. The 0.25 mm taps were aligned and distributed unevenly so as to obtain more data points in regions of large pressure gradients. The C_p distribution and the wake-rake data were read by an automated scani-valve system under computer (HP 9845) control. A hot wire could be installed, as shown, to obtain the spectra of the velocity fluctuations in the wake. Smoke-wire flow visualization was done using a 0.1 mm diameter vertical wire installed about 1 m upstream of the airfoil.

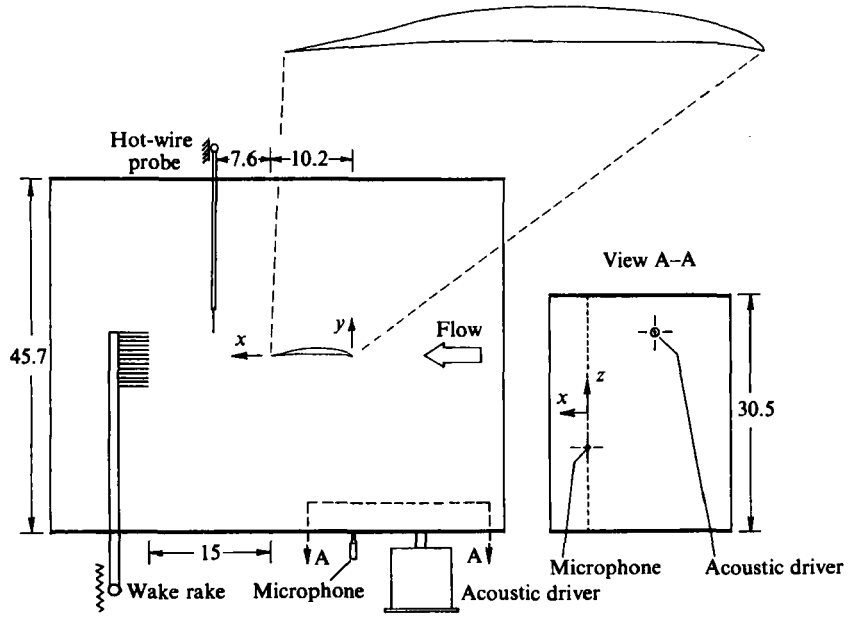

FIGURE 1. Schematic of the test section. Dimensions are in cm.

3. Results and discussion

The lift-coefficient C_l variation as a function of the angle of attack α is shown in figure 2 for two Reynolds numbers (Re_c). Most of the sound excitation data were acquired at the lower Re_c ($=4\times10^4$), at which up to about $\alpha = 8°$, C_l is comparatively low and its variation is also marked by a kink around $\alpha = 8°$. The lower C_l values, or the '*sag*' *in the lift curve*, are associated with an upper-surface laminar separation, as will be made clear shortly with the help of flow-visualization pictures. This is a peculiarity that an airfoil experiences at low Re_c, and is accompanied by a drastic drop in C_l/C_d (see figure 2 of Lissaman 1983; Carmichael 1981). With increasing Re_c, depending on the ambient disturbances, early transition in the boundary layer or the separated shear layer keeps the flow attached, resulting in the improved lift coefficient. In the range $\alpha \lesssim 8°$, significant further improvement in C_l is not expected as Re_c is increased further. At the higher Re_c ($=10^5$), another peculiarity, in the form of a dip in the C_l curve, occurs in the α-range of 8°–15°; the reason for this is not clear but it could be associated with a Reynolds-number dependence of the 'separation bubble'.

Measurements with increasing or decreasing α, at both the Re_c values, did not reveal any hysteresis in the C_l variations. This is unlike the situation with some other low Re_c airfoils, where a hysteresis loop in the C_l curve is exhibited (see e.g. Mueller 1985). The relatively high turbulence intensity in the tunnel (about 0.25 %) could be a reason why it was not observed (Marchman, Sumantran & Schaefer 1987). However, the exact cause remains unknown as hysteresis has been observed under comparable or even higher ambient turbulence levels; on the other hand, the phenomenon is known to depend on other factors like airfoil shape, aspect ratio, Reynolds number, etc. (for a discussion of these effects, see the reference cited above). The absence of hysteresis notwithstanding, acoustic excitation is found to affect the flow over the airfoil dramatically, involving different flow mechanisms in different ranges of α, as described in the following.

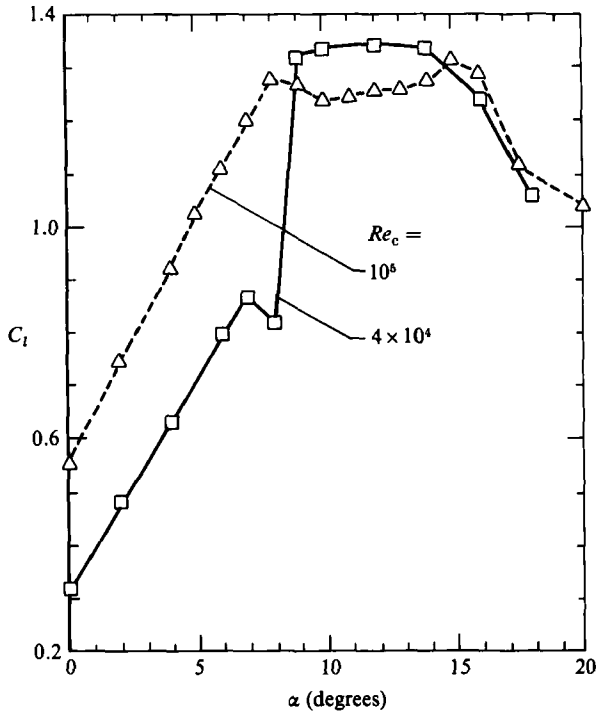

FIGURE 2. Lift-coefficient C_l variation with angle of attack α.

First, the tunnel resonance characteristics, as monitored by the sound pressure level at the microphone location L_R, are documented in figure 3. These data are obtained by varying the excitation frequency f_p in discrete steps while keeping the input voltage to the acoustic driver a constant. The first peak in this graph, at 182 Hz, is believed to be associated with the fundamental, longitudinal resonance of the test section, while the peak at 376 Hz is verified to be the fundamental cross-resonance in the vertical direction (see §3.1). In view of the non-ideal resonating conditions, i.e. the particular sound source in use, the details of the tunnel geometry, the presence of the airfoil, etc., it is impossible to ascertain the nature of the standing waves corresponding to all the peaks in this graph. The cross-resonances turned out, however, to have a profound influence on the flow-excitation results, as discussed in §3.1.

The variation of C_l with f_p is shown in figure 4 for $\alpha = 18°$. The data are normalized by the corresponding lift coefficient for the unexcited flow C_{l0}. For all data, L_R was held constant at 104 dB. One observes that the lift coefficient can indeed by increased substantially, and that despite L_R having been held constant, the C_l variation is marked by the strong peaks. The latter trend is due to the influence of the cross-resonances, which is discussed in detail in §3.1.

The C_l variation was similarly measured for other angles of attack, at $Re_c = 4 \times 10^4$, and the results are shown in figure 5. Note that the abscissa is logarithmic, the curves are staggered vertically, and that the vertical scale is the same for all curves. The arrows indicate the most prominent change in C_l from the unexcited level (the base of each arrow represents corresponding $C_l/C_{l0} = 1$). Inspection of the data makes it apparent that the sound excitation affects the flow in distinct ranges of frequencies for different ranges of α. The influence of tunnel

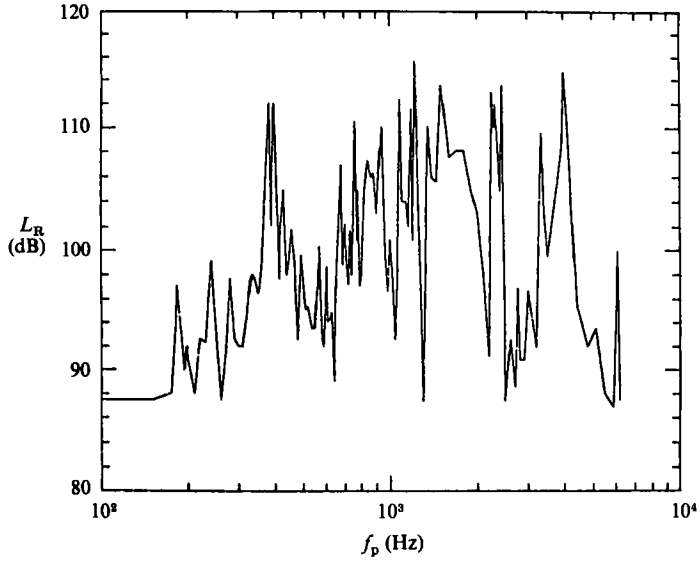

FIGURE 3. Tunnel resonance characteristics: L_R *vs.* f_p for constant input voltage to the acoustic driver.

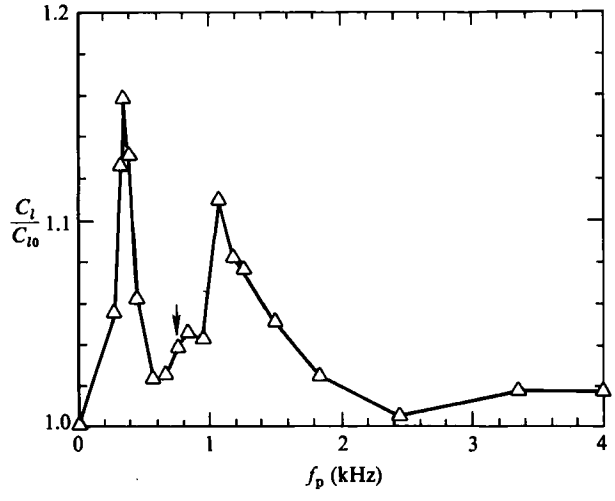

FIGURE 4. C_l variation with excitation frequency f_p. Reference sound pressure level, $L_R = 104$ dB; $\alpha = 18°$. C_{l0} is the lift coefficient for the corresponding unexcited flow; $Re_c = 4 \times 10^4$.

resonance on some sets of data is also apparent. In the range $\alpha \lesssim 8°$, a large (relative) increase in C_l takes place for low frequencies of excitation. Note that the lowest f_p was limited by the acoustic-driver characteristics, and the data trends suggest a continued effect at even lower f_p values. Note especially that for $\alpha = 8°$ the improvement (as much as 50 % increase) is achieved whether the excitation frequency corresponds to a tunnel resonance or not. Small-amplitude excitation was sufficient to produce the desired effect, as confirmed by the data in figure 6. Thus, the laminar separation on the upper surface, occurring in the low-α cases, could be removed by the choice of a relatively low f_p within a range. The corresponding Strouhal number $St = f_p c/U_\infty$ ranged from about 5 to 1, and probably lower. It is worth noting here

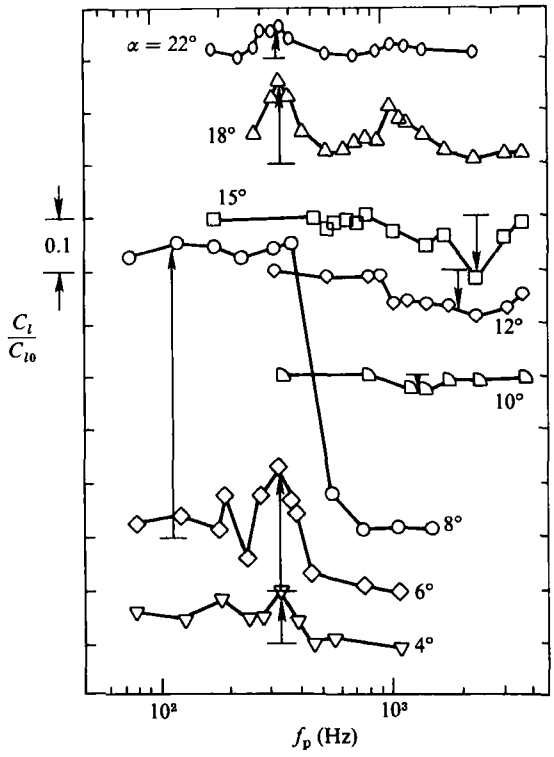

FIGURE 5. C_l variation with f_p for various α. $L_R = 104$ dB for all data; $Re_c = 4 \times 10^4$.

that the sensitivity of the lift-curve 'sag' to small-amplitude disturbance may partly explain large discrepancies in the performance of certain low-Reynolds-number airfoils when measured in different wind tunnels (E. Reshotko, private communications; see Carmichael 1981 who also reported (DELFT) data showing removal of the 'sag' by a 300 Hz tone).

In the α-range of 10°–15° (figure 5), practically no improvement in C_l could be achieved. Instead, for certain high f_p values, a decrease in C_l took place. The aerodynamics and sound interaction at $\alpha \approx 15°$ will be discussed separately in §3.2.

The excitation-amplitude effect is shown in figure 6. For each of three angles of attack C_l *vs.* L_R data are shown for two f_p values. For $\alpha = 8°$, amplitudes only a few dB higher than the background level cause a large increase in C_l, with no further increase for increasing L_R. For post-stall cases, e.g. at $\alpha = 18°$, however, a strong amplitude dependence is observed; the higher the amplitude of excitation the larger the increase in C_l – an observation also made by Ahuja & Burrin (1984). (In our discussion, 'stall' denotes the rapid decrease in C_l with increasing α, involving separation from the leading edge, commencing roughly at $\alpha = 16°$.) A relatively weaker amplitude dependence is observed for the pre-stall case at $\alpha = 15°$, the decrease in C_l levelling off within the measurement range of L_R.

Figure 7 shows smoke-wire visualization pictures, the flow being from right to left in all cases. For each α, there is a pair of pictures – the one on the right for a representative, 'effective' excitation case, and the one on the left for the corresponding unexcited flow. Consider the unexcited flows with increasing α. For $\alpha = 4°$, there is an attached laminar boundary layer on the upper surface, and

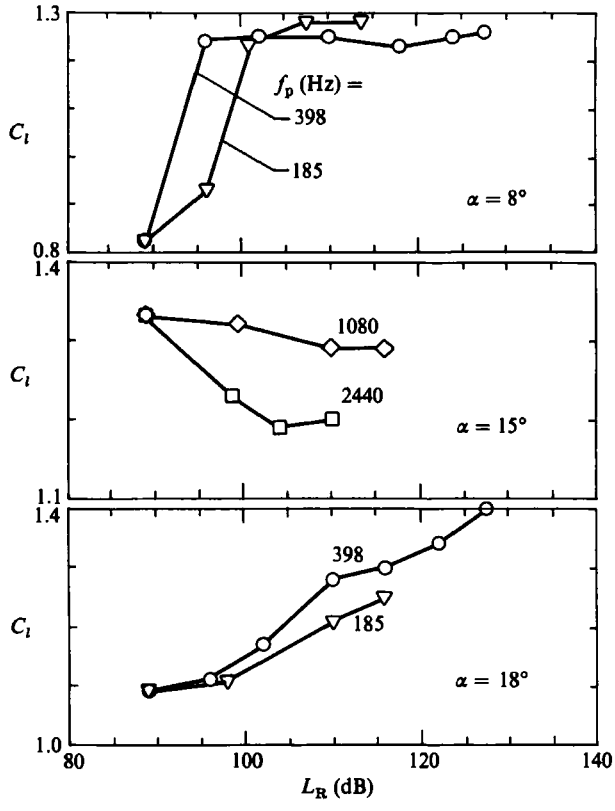

FIGURE 6. Amplitude effect on C_l; $Re_c = 4 \times 10^4$.

separation occurs around the 65% chord location. With increasing α the point of separation moves upstream, until at 8° there is separation practically from the leading edge. This is the α-range where C_l is unusually low (figure 2). As α is increased further, the separated shear layer reattaches, resulting in a sharp increase in the C_l. Presumably, the reattachment occurs as the separated shear layer is energized after undergoing transition. This would then be the situation where a 'separation bubble' would be expected near the leading edge. However, such a bubble could be small, occupying only a few percent of the chord (Mueller & Batill 1982), and is not clearly visible in the picture for $\alpha = 10°$. In the picture for $\alpha = 12°$, however, a small bubble is quite evident.

With further increase in α, just prior to stall ($\alpha \approx 15°$), a low-frequency oscillation was observed in the wake, which will be discussed in §3.2. Still further increase in α resulted in separation from the leading edge, marking the beginning of stall.

The effect of excitation should be clear in the flow-visualization pictures for at least a few cases. The removal of the laminar separation at $\alpha = 8°$ ought to be evident; so should be the narrowing of the wake at $\alpha = 18°$. A dramatic narrowing of the wake is also clear for $\alpha = 15°$, seemingly associated with the elimination of large-scale, vortical structures.

The velocity profiles in the wake are shown in figure 8, with and without excitation, for three angles of attack. Representative cases of excitation producing large effects have been shown. A narrow wake with a smaller velocity defect is achieved in all cases, yielding a drop in the drag. Profile drag was computed, using Jones' method,

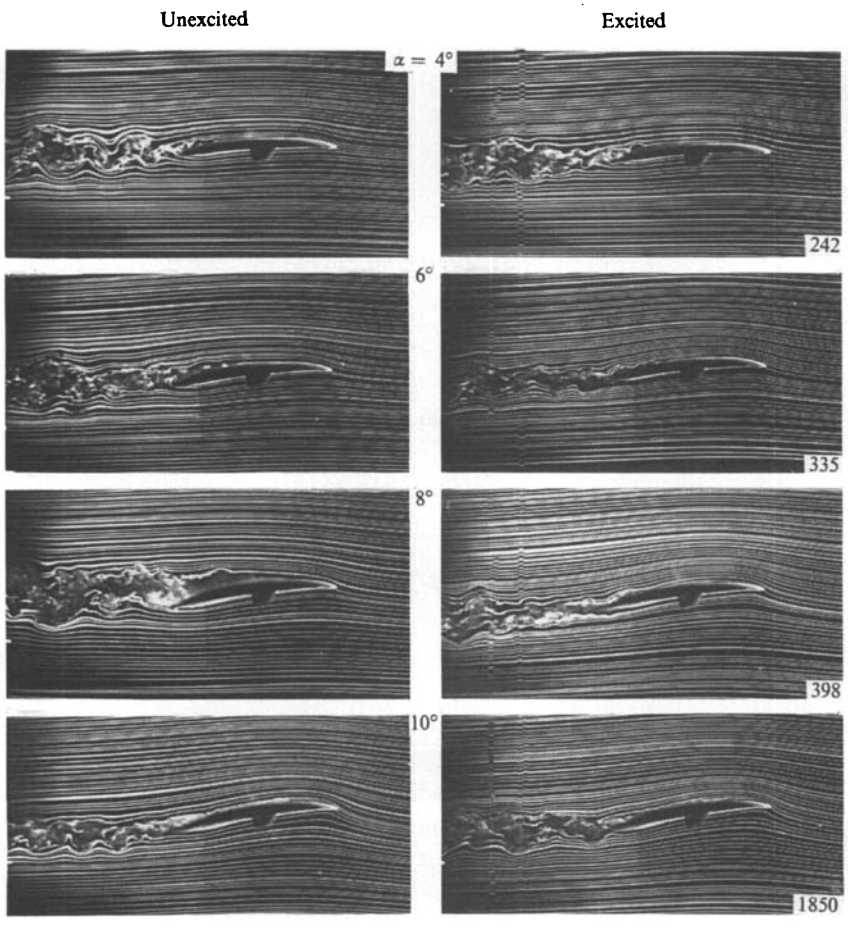

FIGURE 7(a). For caption see facing page.

(Schlichting 1979, p. 761). Note that the measurement station was 1.5 chord lengths downstream of the trailing edge, and that the velocity 'overshoots' on the edges were negligible. Thus, in our calculation, Jones' method reduced to a straightforward evaluation of the momentum defect from the wake profiles. However, there are questions as to the accuracy of the C_d data obtained by wake-rake measurements at low Re_c (see e.g. Mueller 1985); but the comparison of the data with and without excitation to evaluate the relative changes should be quite valid. Thus, only data for C_l/C_d as a function of f_p are shown (figure 9) for the three-values of α of figure 8. For $\alpha = 6°$ and 18°, C_l/C_d is found to increase in the same f_p range where C_l values increase, with a corresponding decrease in C_d. (C_d *vs.* f_p data can be inferred from figures 5 and 9.) For $\alpha = 15°$ one finds that the decrease in C_d is so large that a net increase in C_l/C_d is produced, even though C_l values decreased.

Examples of C_p distributions with and without excitation are documented in figure 10. The short-dashed curve in each case represents the unexcited flow, f_p values being indicated for each excitation case. The long-dashed curve for $\alpha = 8°$ was obtained by an (inviscid) numerical code in connection with stability analysis. Similar C_p distributions were integrated to obtain the C_l data of figure 5. Note that the data at the leading and the trailing edges are artificially generated, but (in view of the

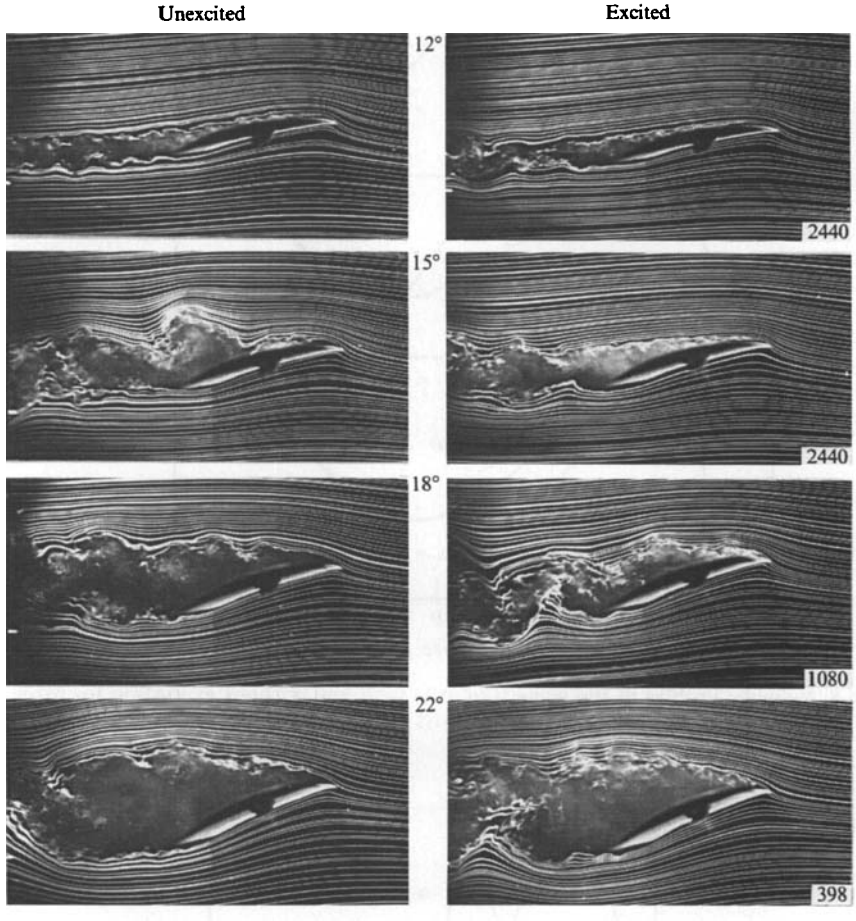

FIGURE 7. Smoke-wire flow-visualization pictures for various α, with and without excitation; $Re_c = 4 \times 10^4$, $L_R = 104$ dB, and f_p (Hz) is indicated on lower right corner for each excitation case.

sharp edges) the error in C_l due to this is negligible. The excitation cases are found to induce profound redistributions in C_p, presumably due to the changes in the separation characteristics. Similar changes in C_p distribution under sound excitation were also observed by Ahuja & Burrin (1984).

In all excitation cases, there is a large increase in the 'suction peak' near the leading edge on the upper surface, even when C_l decreased at $\alpha = 15°$. The static pressure at the 5% chord location on the upper surface (C_{p2}), roughly representing the amplitude of the 'suction peak', is shown in figure 11 for a few α values as a function of f_p. We observe that a large relative increase occurs, especially at the higher angles of attack. The C_{p2} values are also found to increase in the same f_p range where C_l/C_d shows an increase. It is interesting that monitoring a single static pressure near the 'suction peak' essentially reflected on the optimum excitation parameters in all the cases. Thus, although the dynamics is not clear, such a simplified measurement seems attractive for diagnostic purposes in similar future experiments or applications.

The effect of acoustic excitation at a higher Reynolds number ($Re_c = 10^5$) is shown in figure 12. Data similar to those of figure 5 are shown for $\alpha = 15°$ and 18°. In this case no dramatic effect occurs at small angles, as is to be expected. For $\alpha = 18°$, the

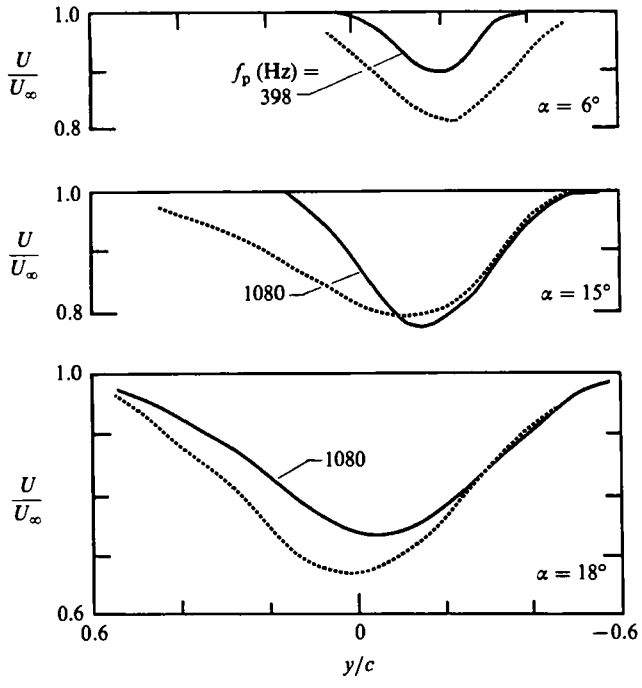

FIGURE 8. Velocity profiles in the wake (figure 1) with and without excitation for three values of α. $L_R = 104$ dB; $Re_c = 4 \times 10^4$.

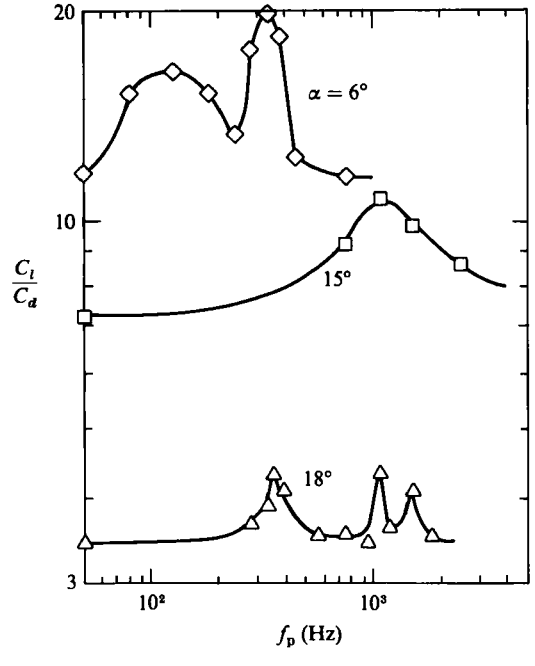

FIGURE 9. C_l/C_d variation with f_p. $L_R = 104$ dB; $Re_c = 4 \times 10^4$. Left-most data points are artificial and represent respective unexcited levels.

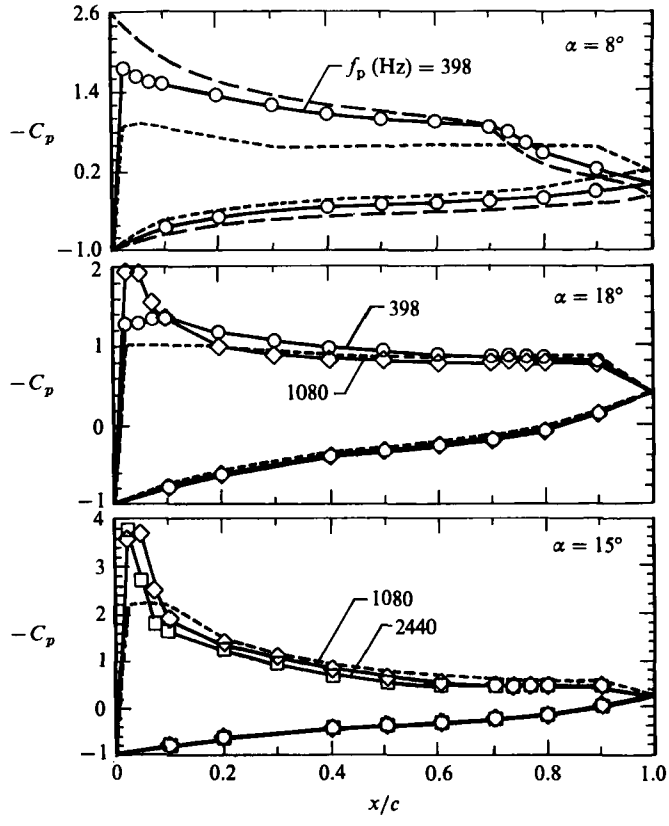

FIGURE 10. C_p distribution around the airfoil. Short-dashed curves for unexcited flow. Long-dashed curve for $\alpha = 8°$ represents numerical analysis prediction. $L_R = 104$ dB; $Re_c = 4 \times 10^4$.

effect of the tunnel resonance at 1080 Hz is apparent; however, the band of effective frequencies has shifted to a higher *St*-range of about 6–60, relative to the *St*-range of about 4–25 found effective for the $Re_c = 4 \times 10^4$ case. Similarly, for $\alpha = 15°$, the decrease in C_l is also observed, in a higher range of f_p; in this case, the approximate effective *St*-ranges are 7–70 and 10–120 for $Re_c = 4 \times 10^4$ and 10^5, respectively.

3.1. *Effect of tunnel resonance*

Referring back to figure 4, one notes that the two prominent peaks in the C_l variations occurred at 376 Hz and 1080 Hz. These two correspond to the fundamental and the second harmonic of the cross-resonance between the floor and the ceiling of the test section, as confirmed by the data shown in figure 13(*a*). A $\frac{1}{4}$ in. microphone was traversed inside the test section (with no flow). Figure 13(*a*) shows the variation of the sound pressure level with the vertical distance, measured a half-chord upstream of the airfoil and at mid-span, for three f_p values. The number of nodes shows that 376 Hz represents the fundamental cross-resonance in the vertical direction, and 758 Hz and 1080 Hz are its first and second harmonics. Small changes in the excitation frequency resulted in the disappearance of these standing waves. For each f_p, spanwise traverse at two heights showed essentially uniform amplitude variation (not shown). Note that the two higher frequencies are not exact multiples of the fundamental; the reason for this could not be determined. (Differences between

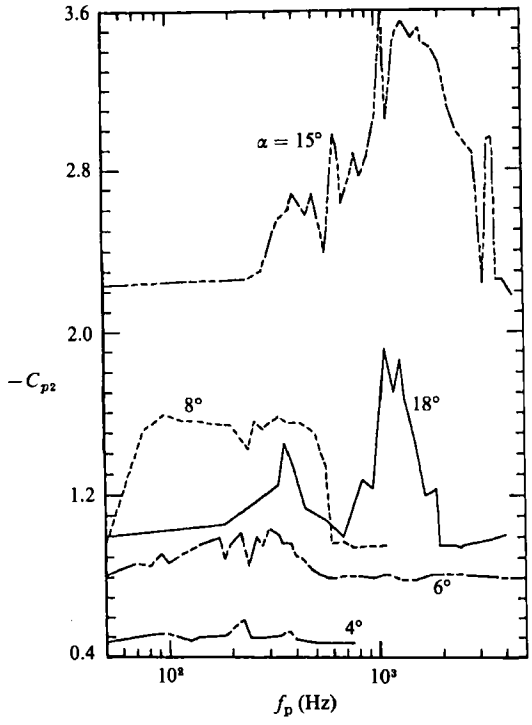

FIGURE 11. Variation of static pressure, at the 5% chord position on upper surface, with f_p. $L_R = 104$ dB; $Re_c = 4 \times 10^4$. Curves are artificially terminated on the left at respective unexcited levels.

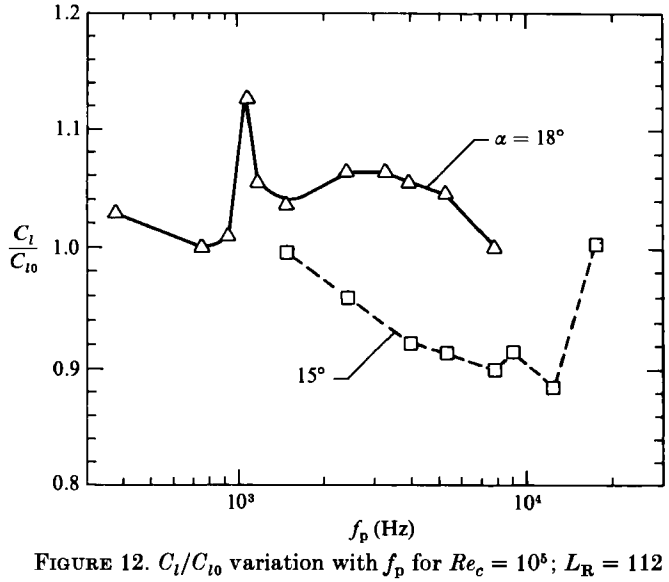

FIGURE 12. C_l/C_{l0} variation with f_p for $Re_c = 10^5$; $L_R = 112$ dB.

predicted and observed higher harmonics in cross-resonance were also reported by Parker 1966.) Also remaining unexplained are such features as the occurrence of a closely spaced resonance at 398 Hz (figure 3). Vertical traverse at 398 Hz showed a similar sound pressure level variation as for the 376 Hz case, although half-wave resonance predicts a fundamental close to 376 Hz. As discussed before, some of these

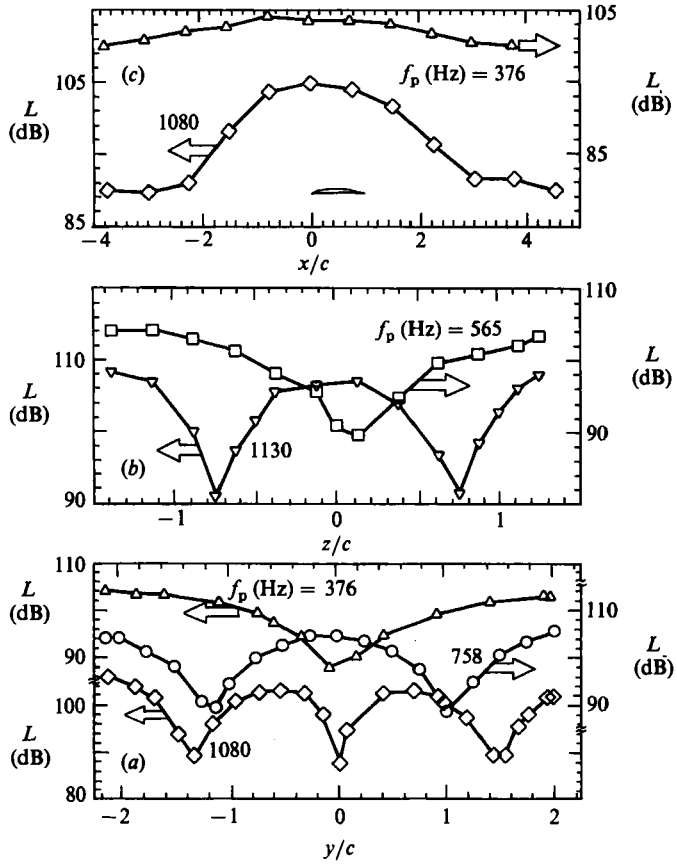

FIGURE 13. Sound-pressure-level L variation inside the test section for different f_p; $L_R = 104$ dB (see figure 1 for coordinates). (*a*) variation with height $z/c = 0$, $x/c \approx -0.1$; (*b*) spanwise variation $y/c = 0$, $x/c \approx -0.1$; (*c*) axial variation $z/c = 0$, $y/c \approx -2.15$.

discrepancies could be due to the non-ideal resonating conditions inevitable in a wind tunnel.

The fundamental and the first harmonic of the spanwise cross-resonance are documented in figure 13(*b*), while the axial variation of the amplitude at 376 Hz and 1080 Hz is shown in figure 13(*c*). The relative size and position of the airfoil are shown in the latter figure, and it is clear that even for 1080 Hz the amplitude does not vary appreciably over the extent of the airfoil.

The above cross-resonances are expected from duct-acoustic calculations. The frequency of the mode with m nodes in y and n nodes in z is given by for example Goldstein (1976):

$$f_{mn} = \frac{a_0}{2\pi}\left[1-\left(\frac{U_\infty}{a_0}\right)^2\right]^{\frac{1}{2}}\left[\left(\frac{m\pi}{H}\right)^2+\left(\frac{n\pi}{W}\right)^2\right]^{\frac{1}{2}},$$

where a_0 is the ambient sound speed, H the height and W the span of the test section. The boundary conditions dictate that the pressure and velocity due to a standing wave be 180° out of phase, and that the component of the velocity fluctuation be determined by the direction of the reflecting sound waves. Thus, a u fluctuation is induced by longitudinal standing wave and v' and w' fluctuations by the appropriate

cross-resonances, u', v' and w' being the streamwise, height-wise and spanwise velocity components respectively. For 376 Hz, one would thus expect large v' fluctuation at mid-height, corresponding to the pressure node. This was qualitatively checked with a hot wire (no-flow condition); the r.m.s. amplitude of the hot-wire output did have a maximum at mid-height, gradually falling off towards the ceiling and the floor.

The expected velocity-fluctuation patterns for the standing waves at 376 Hz and 1080 Hz are sketched in figure 14 (*a*, *b*) respectively. The solid lines represent regions of v' maxima while the broken lines represent regions of w' maxima, each line being also a region of pressure minimum. It becomes apparent that at both 376 Hz and 1080 Hz, which yielded the two peaks in C_l variation, there is a region of v' maximum at mid-height where the airfoil is located. The same could be inferred about a similar set of data obtained by Ahuja & Burrin (1984) exhibiting a C_l maximum at 665 Hz. The 25 cm × 75 cm test section of their tunnel ought to yield a standing wave at about 665 Hz, as sketched in figure 14 (*c*). It is interesting to note that, even in the absence of any artificial excitation, both Davis (1975) and Parker (1966) had observed vortex shedding from an airfoil or a flat plate to 'lock-on' to the cross-resonances of their tunnels. In particular, Parker observed a strong resonance condition when the pressure nodes coincided with the flat plates, a situation when large transverse velocity fluctuation would be expected around the plates.

In figure 14 (*b*), the second harmonic in the vertical direction is shown to coincide with the first harmonic in the spanwise direction because of the width-to-height ratio of the test section. Measurements showed, however, that the latter occurred at a slightly higher frequency, most probably owing to non-ideal conditions, as discussed earlier. This, however, is inconsequential in the present discussion. The present data indicate that the most effective excitation takes place whenever a large v' fluctuation is induced. Recall, from figure 4, that the spanwise resonances at 565 Hz and 1130 Hz did not result in significant increases in C_l. However, the spanwise resonances induced large w' only in localized regions. It is probable that equally effective excitation would take place if large w' were induced uniformly over the entire span, as in the case of v' antinodes.

The above results provide a clearer insight into the role played by the tunnel resonance in exciting the separated flow. Clearly, conditions inducing large transverse velocity fluctuations near the airfoil are most successful in the excitation, and thus produce the observed increase in C_l. But subjecting the airfoil to excessive sound pressure level may not necessarily produce the desired effect. For example, compare the sound pressure levels at mid-height for the three frequencies of figure 13 (*a*). One finds that only 87 dB at 376 Hz and 1080 Hz was required to increase C_l by 16 % and 11 % respectively, while the corresponding increase at 758 Hz, marked by an arrow in figure 4, was only 5 % despite the sound pressure level being 17 dB higher.

The above results also raise a question about the suitability of the sound pressure level at the floor L_R, or for that matter anywhere in the test section, as an adequate reference parameter in the study. However, the choice of such a parameter, in order to differentiate the aerodynamics from the resonance effects, is far from clear. For example, a sound pressure level read from a suitable flush-mounted microphone on the airfoil surface will not only be affected by the tunnel resonances but also by the separated flow. It would seem that the velocity fluctuation near the leading edge could be a better parameter, provided that one also ensures the same (or similar) resonance modes at all frequencies. One could design an experiment to this end, e.g.

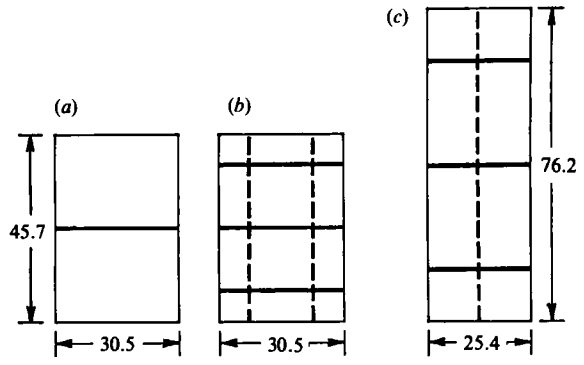

FIGURE 14. Estimated standing-wave nodes inside the test section. Solid lines for regions of v' maxima, broken lines for regions of w' maxima. (*a*) and (*b*) for the present case correspond to $f_p = 376$ Hz and 1080 Hz respectively. (*c*) The experiment of Ahuja & Burrin (1984) at $f_p = 665$ Hz. Dimensions in cm.

by providing for variation in the test-section dimensions as f_p is varied, but a foolproof scheme seems difficult indeed.

The difficulties in deciphering the aerodynamics of sound-excited flows, especially in a wind tunnel, may be considered further. One begins to appreciate this difficulty from the fact that a kaleidoscope of nodal patterns, as in figure 14, would result if only f_p is varied; one then has to consider scattering by the airfoil, influence of the flow, etc. Pfenninger's (1977) experiment is another example of standing waves of a different nature inducing boundary-layer transition; an 'internal' standing wave was set up inside a duct connecting the suction slots of his airfoil, which, in contrast to the present case, most effectively excited the boundary layer at regions corresponding to the pressure *anti*nodes. (However, it is reasonable to believe that these antinodes corresponded to regions where the transverse velocity through the suction slots was of maximum amplitude, thus once again emphasizing the importance of the cross-stream velocity in the excitation mechanism.) Even in the absence of tunnel resonance, an example of how the flow itself may interact with the sound field to set up a 'standing-wave' pattern is Leehey & Shapiro's (1977) boundary-layer experiment; a streamwise interference pattern is observed by them, due to the difference in the phase velocities of the exciting sound wave and the resulting Tollmien–Schlichting waves. In passing, it is worth emphasizing that in calculating the fluid-particle velocity due to an imposed sound field, such as was done in the receptivity experiments of Gedney (1983) and Aizin & Polyakov (see Nishioka & Morkovin 1985), one must carefully avoid, or duly consider the presence of, any such standing wave.

In spite of the above difficulties, the present and previous results have amply demonstrated that separation control by sound excitation is quite possible. The tunnel cross-resonances act only as conduits through which the excitation induces large-amplitude velocity fluctuation, resulting in a more effective separation control. It is needless to emphasize, however, that the tunnel resonances are not necessary conditions, as some velocity fluctuation occurs at other frequencies too, resulting in various amounts of increase in the lift. The observed resonance effects suggest, however, that alternative methods specifically inducing cross-stream velocity perturbation may be more viable in the excitation of the flows under consideration.

3.2. *Pre-stall, organized flow structure*

As mentioned earlier, we noted a rather remarkable organized flow structure in the airfoil wake just prior to stall at $\alpha = 15°$. This was inferred from (hot-wire) velocity-spectra measurements in the wake, examples of which are shown in figure 15. The four upper traces are for the flow without excitation. The uppermost trace corresponds to $Re_c = 4 \times 10^4$ while the fourth from top corresponds to the highest Re_c ($= 1.4 \times 10^5$) covered in the present investigation. A low-frequency, sharp peak clearly appears in the spectra, indicating a periodic vortex-shedding-like motion in the wake. The frequency of the spectral peak (in Hz) is also indicated; limited hot-wire traverses, in the streamwise direction over 0.5–1.0 chord lengths as well as across the wake, showed the frequency to remain unchanged for a given U_∞.

It is evident that the frequency (f_m) of the spectral peak scales with U_∞, and the Strouhal number ($f_m c/U_\infty$) based on the chord length is about 0.07 in all cases. Note that the corresponding hydrodynamic wavelength, assuming a convection velocity of U_∞, is about 14 chord lengths. Thus, the photograph for $\alpha = 15°$ in figure 7 is far from capturing one full wavelength corresponding to the 4.5 Hz oscillation.

A number of previous experiments dealt with vortex shedding, trailing-edge noise, etc. from airfoils. What is intriguing here is that the corresponding non-dimensional frequencies are much lower than those in any of these previous studies. For example, Davis (1975) observed trailing-edge noise at a modified Strouhal number, based on the trailing-edge thickness with boundary-layer correction, of about 0.21. In the present case, even if the projected width obstructing the flow (i.e. $c \sin 15°$) is taken as the lengthscale, the corresponding Strouhal number is only 0.02. At much lower Re_c ($\lesssim 8000$), Cendenese, Cerri & Iannetta (1981) reported a (quasi-)periodic wake flow, rather similar to the present case, but still occurring at a much higher St of about 0.3. Brooks & Schlinker (1983) reported the vortex-shedding Strouhal number, at various α, to vary as $0.011 Re_c^{\frac{1}{2}}$; the shedding mechanism in the present case must be different, because no Re_c dependence is observed. An elegant study of vortex shedding from a variety of bluff bodies has been done much earlier by Roshko (1954). He showed that a modified Strouhal number, $St^* = St\,\xi/k$, was the same, about 0.16, in all the cases. Here, k is related to the pressure coefficient at the separation point by $C_p = 1 - k^2$, and ξ is an empirical factor depending on k. Using C_{p2} ($= -2.2$) from figure 10, and invoking figure 7 of Roshko's paper, a value of only 0.01, as opposed to 0.16, is obtained for St^* in the present case.

Note that the very low frequency and its continuous variation with U_∞ lead to the belief that the phenomenon may not be linked to any standing-wave mode of the tunnel. Free-stream turbulence as well as background sound pressure spectra were also free from any such peaks. The fan rotational speed appeared a plausible driving mechanism, but was also ruled out because the corresponding frequency was about 2.5 times higher and varied nonlinearly with U_∞. Of course, an organized wake structure like this is not only of academic interest but also of concern in application, since it is associated with a decrease in C_l/C_d and may induce undesirable structural vibrations. Thus we felt obliged to report the phenomenon, even though time and facility limitations did not permit us to explore the mechanism any further. The mechanism has essentially remained unexplained, although one could speculate that its origin can be traced to a (periodic) bursting of the separation bubble and the associated instability. (The authors became aware in the final stages of this study that a recent numerical study on airfoil wakes encountered similar low-frequency oscillations; see Rumsey (1987). Specifically, calculations for a NACA 0012 airfoil,

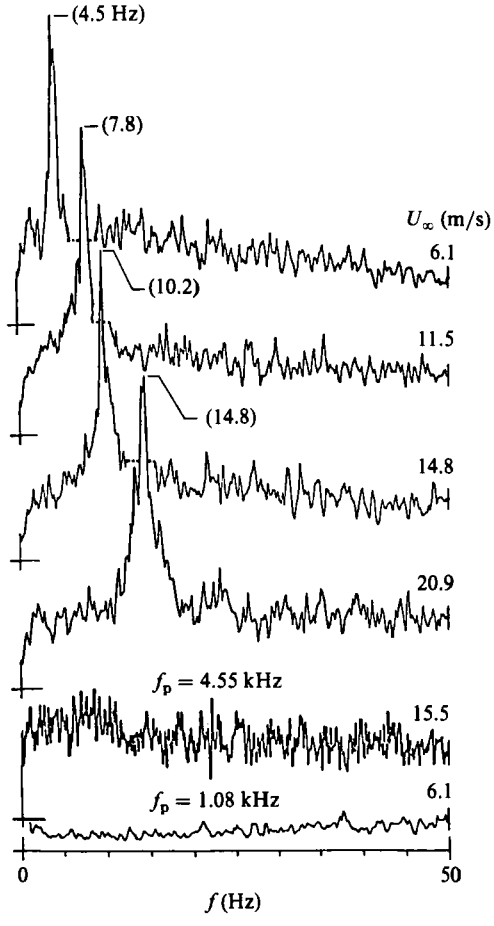

FIGURE 15. Hot-wire velocity spectra measured in the wake (figure 1) for $\alpha = 15°$. The four upper traces are for unexcited flow at the indicated free-stream velocities U_∞. The lower two traces are for excitation at the indicated f_p values. The relative (linear) vertical scales for traces starting from the bottom are: 1.0, 1.0, 0.075, 0.075, 0.10 and 0.225 respectively.

assuming turbulent boundary layers, at $\alpha = 10°$ and $Re_c = 10^6$, yielded a resultant Strouhal number based on chord of 0.097.)

It was discovered, however, that acoustic excitation at an appropriate high frequency could be used to eliminate this shedding completely. This is demonstrated by the lower two traces of figure 15. Note that this elimination is associated with a drop in the C_l (see figures 5 and 12). It was also observed that the f_p range resulting in the removal of the spectral peak approximately coincided with the f_p range yielding the decrease in C_l. The excitation Strouhal number producing the optimum effect is found to be high, and increases with increasing U_∞; for example it is about 18 and 30 in the two cases shown in figure 15. On a closer scrutiny, with the relative vertical scales indicated in the figure caption, it should become clear that the broadband turbulence level is also substantially reduced by the acoustic excitation.

It is interesting that the excitation effect appears morphologically similar to the phenomenon of 'turbulence suppression' in free-shear flows (Zaman & Hussain 1981), in which energetic vortices are also eliminated (or weakened) by high-frequency excitation. The latter requires f_p scaling as the initial shear-layer momentum

thickness, and thus as $U_\infty^{\frac{3}{2}}$; the limited data in the present case also indicate a similar scaling for f_p. Note that while Zaman & Hussain's results apply to simple free-shear layer, the acoustic interaction in the present case is compounded by the presence of the airfoil. It seems likely that the effect on the separated shear layer commences in the vicinity of the leading edge (see the pair of pictures for $\alpha = 15°$ in figure 7), with a possibility that a separation bubble with unsteady behaviour is eliminated by the excitation. We note in passing that a similar mechanism might explain a curious effect, observed long ago by Mechel, Mertens & Schilz (1963), of turbulence suppression in a flat-plate boundary layer by acoustic excitation.

The 'weakening' of the large-scale vortical structures by the high-frequency excitation provides an explanation for the observed decrease in C_l. While excitation typically energizes the separated shear layer, causing a tendency towards reattachment and thus an increase in C_l, in these specific cases the separated shear layer is actually de-energized, thus bringing in the reverse effect. Lift is thus decreased; however, there is an associated reduction in drag as manifested by a narrowing of the wake, the net result being a favourable increase in C_l/C_d.

3.3. *Stability analysis*

Whether the imparted sound wave excited the boundary layer or the separated shear layer was one question posed at the beginning of the study. An answer was sought by carrying out a stability analysis of the boundary layer around the airfoil, with the intent of comparing predicted unstable frequencies with experimental f_p ranges producing the optimum effect. This was done by available numerical codes in the NASA Langley software library.

The EPPLER–SOMERS code provided the C_p distribution, via a 'panel method', having taken the airfoil coordinates as input. From this C_p distribution, the CEBECI–KAUPS code then provided the boundary-layer parameters around the airfoil for a given flow configuration. The code SALLY was then used to obtain growths of given disturbances having various frequencies and wavenumbers. Details of the first code are given by Eppler & Somers (1980), and the methods involved in the latter two are discussed by Srokowski & Orszag (1977).

While the calculated C_p distribution for $\alpha = 8°$ was shown in figure 10, the EPPLER–SOMERS-code prediction for the momentum thickness θ on the upper surface is shown in figure 16. For clarity, the abscissa (chordwise distance) has been shown with its origin at the stagnation point. For the higher angles of attack, the sharp rise in θ represents separation, near the leading edge (formally predicted in the code by the shape-factor variation). Attached laminar-boundary-layer flow over a reasonably long chordwise distance is predicted for $\alpha \lesssim 6°$. *Only in the latter situation*, the boundary layer remains attached to become unstable, and the stability analysis is expected to yield unstable modes. However, our analysis, carried out for $Re_c = 4 \times 10^4$, showed that the boundary layer before separation was *stable at all angles of attack*.

Of course, questions remain as to the applicability of the predictions; for example, while linear stability has been considered, it is likely that nonlinear effects may be coming into play. Another consideration in the problem at hand is the separated-shear-layer instability. The stability characteristics of a *free*-shear layer are well documented and successfully analysed (e.g. by Michalke 1965), but it is not appropriate to compare those results here, because the presence of the solid boundary cannot be ignored. Notice that the purpose of the excitation is to force reattachment, and thus the stability problem must include the boundary, the separation bubble,

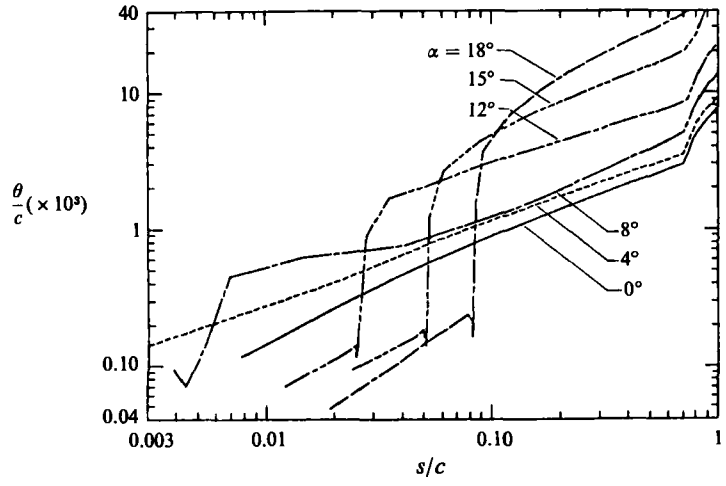

FIGURE 16. Predicted momentum thickness variation with chordwise distance on the upper surface, from stagnation point; $Re_c = 4 \times 10^4$.

etc. A satisfactory analytical treatment of the complete phenomenon is not yet available. However, the 'receptivity' of a shear layer separating from a blunt body has been considered by Goldstein (1984). (The reader may refer to Crighton 1981 for a discussion of pertinent analytical aspects of flow acoustic interaction.) Goldstein's analysis provides an expression for the 'coupling coefficient' between the imposed disturbance and the resulting instability wave (see also Tam 1978), and it was observed that disturbances in the limit $St \ll Re_c^{\frac{1}{2}}$ ought to be effective in the excitation. (A lower frequency limit of $Re_c^{\frac{1}{4}} \ll St$ applies to his analysis.) The analysis is for separated flow from a smooth surface, and thus may be expected to apply only for the low-α cases in our experiment. We note that for the $\alpha \lesssim 8°$ cases, the upper limit of the Strouhal-number range found effective in the excitation ($St \approx 5$, see figure 5), falls well within the limit of $Re_c^{\frac{1}{2}}$ (≈ 14); excitation at higher frequencies is completely ineffective. This qualitative agreement of the effective upper frequency limit with Goldstein's observation lends further support that the excitation mechanism indeed hinges on the instability of the separating shear layer.

Finally, it should be recognized that there is sufficient evidence of acoustic excitation amplifying the boundary layer Tollmien–Schlichting waves leading to transition, e.g. as observed by Pfenninger (1977) on a swept airfoil at $Re_c = 6 \times 10^6$. However, based on the above considerations, one must infer that excitation of the upstream boundary layer is not always the mechanism by which 'acoustic tripping' takes place. Excitation of the shear layer, perhaps, near the point of separation, seems a far more likely mechanism in the observations of the present and many other previous experiments.

4. Conclusions

Acoustic excitation is found to significantly influence the flow separation over an airfoil, at low Reynolds numbers. The effect and the corresponding flow mechanisms are observed to be different in different ranges of the angle of attack. For $\alpha \lesssim 8°$, a laminar separation on the upper surface, otherwise drastically degrading the airfoil performance, is removed readily with a relatively low-frequency excitation.

Excitation frequencies in the range $St \lesssim 5$ are found to be effective at $Re_c = 4 \times 10^4$, amplitudes only a few dB above the background level being sufficient to produce the effect. For $\alpha \gtrsim 18°$, during post-stall, significant increase in C_l (and C_l/C_d) is also achieved, but with large-amplitude excitation, the increase depending directly on the amplitude. The effective St-range in this case is higher, e.g. about 4–25 at $Re_c = 4 \times 10^4$, and is found to increase with increasing Re_c.

A low-frequency, periodic wake flow structure is observed just before stall throughout the Re_c range covered. The phenomenon appears unique in that the corresponding non-dimensional frequency is about an order-of-magnitude lower than that reported in any previous study dealing with vortex shedding from bluff bodies. It has also been found that excitation at a high frequency, apparently scaling as $U_\infty^{\frac{3}{2}}$, completely eliminates this organized flow structure. (At $Re_c = 4 \times 10^4$, excitation in the St-range of about 7–70 produces this effect.) The elimination of the energetic vortical structures from the separated shear layer results in a loss of lift, but a net increase in C_l/C_d.

The tunnel resonance is found to strongly influence the results, especially in the cases requiring large amplitudes. While a similar effect has previously been observed by others, a clear interpretation of the mechanism is provided in the present analysis. It is shown that specific cross-resonances inducing large transverse velocity fluctuations near the airfoil are most effective in the separation control. That a resonance inducing only large-amplitude pressure fluctuations is relatively ineffective delineates the role of the cross-stream velocity fluctuation in the excitation mechanism.

Stability analysis shows that the boundary layer before separation, at the low Re_c, is insensitive to any imposed perturbation. On this basis, it is inferred that the excitation mechanism must hinge on the instability of the separated shear layer. However, the process is likely to be strongly influenced by the presence of the solid boundary, the separation bubble, etc. While a satisfactory analysis of the complete phenomenon is not available, a qualitative agreement between the upper limit of the effective Strouhal number, for $\alpha \lesssim 8°$, and Goldstein's (1984) prediction for the 'receptivity' of similar flows, adds support to the above inference.

In terms of application, acoustic excitation appears promising in the control of laminar separation occurring near the design angle of attack at low Re_c. Should the pre-stall organized vortex shedding be a common phenomenon with other airfoils, acoustic excitation could also be an effective device to suppress that. For post-stall operation, in spite of the tunnel resonance effects, the results have proven that improvement in the airfoil performance is possible. It is conceivable that in certain applications involving enclosures (e.g. a turbine), one could take advantage of the resonance characteristics to achieve improvement of the flow over the blades via a suitable sound source. However, the demonstrated importance of the transverse velocity fluctuations in the excitation mechanism indicates that imparting a beam of sound may not be the best method in free-flight. Controlled induction of velocity fluctuation, perhaps near the leading edge, would appear more effective; localized perturbation devices, like piezoelectric strips or heat strips (Maestrello 1985), thus seem promising in this regard.

Finally, while the present data pertain to low Reynolds numbers, Ahuja & Burrin (1984) have achieved post-stall improvement in performance at relatively higher Re_c ($\approx 10^6$). They found, however, that for a given sound pressure level, the improvement in C_l decreases with increasing Re_c. It remains to be demonstrated that the separation

control can be achieved at much higher Re_c (perhaps through an alternative excitation technique as suggested above).

The authors are grateful to Dr L. Maestrello, Dr J. C. Yu, and Dr M. K. Myers for valuable discussions on the acoustic aspects, and especially to Mr W. D. Harvey for providing encouragement and taking an active interest throughout the course of this study. The research was supported by grants under contract numbers NAS1-17670 and NAS1-17683.

REFERENCES

AHUJA, K. K. & BURRIN, R. H. 1984 Control of flow separation by sound. *AIAA Paper No.* 84-2298.

BROOKS, T. F. & SCHLINKER, R. H. 1983 Progress in rotor broadband noise research. *Vertica* **7**, 287–307.

CARMICHAEL, B. H. 1981 Low Reynolds number airfoil survey: vol. I, *NASA Contractor Report No.* 165803.

CENDENESE, A., CERRI, G. & IANNETTA, S. 1981 Experimental analysis of the wake behind an isolated cambered airfoil. *Proc. IUTAM Symp. Unsteady Turbulent Shear Flows*, pp. 273–284. Springer.

COLLINS, F. G. & ZELENEVITZ, J. 1975 Influence of sound upon separated flow over wings. *AIAA J.* **13**, 408–410.

CRIGHTON, D. G. 1981 Acoustics as a branch of fluid mechanics. *J. Fluid Mech.* **106**, 261–298.

DAVIS, S. S. 1975 Measurements of discrete vortex noise in a closed-throat wind tunnel. *AIAA Paper No.* 75-488.

EPPLER, R. & SOMERS, D. M. 1980 A computer program for the design and analysis of low-speed airfoils. *NASA TM*-80210.

GEDNEY, J. G. 1983 The cancellation of a sound-excited Tollmien–Schlichting wave with plate vibration. *Phys. Fluids* **26**, 1158–1161.

GOLDSTEIN, M. E. 1976 *Aeroacoustics*. McGraw-Hill.

GOLDSTEIN, M. E. 1984 Generation of instability waves in flows separating from smooth surfaces. *J. Fluid Mech.* **145**, 71–94.

LEEHEY, P. & SHAPIRO, P. 1977 Leading edge effect in laminar boundary layer excitation by sound. *Proc. IUTAM Symp. Laminar Turbulent Transition*, pp. 321–331. Springer.

LISSAMAN, P. B. S. 1983 Low-Reynolds-number airfoils. *Ann. Rev. Fluid Mech.* **15**, 223–239.

MAESTRELLO, L. 1985 Active transition fixing and control of the boundary layer in air. *AIAA Paper No.* 85-0564.

MANGALAM, S. M. & PFENNINGER, W. 1984 Wind-tunnel tests on a high performance low-Reynolds number airfoil. *AIAA Paper No.* 84-0628.

MARCHMAN, J. F., SUMANTRAN, V. & SCHAEFER, C. G. 1987 Acoustic and turbulence influences on stall hysteresis. *AIAA J.* **25**, 50–51.

MECHEL, F., MERTENS, P. & SCHILZ, W. 1963 Research of sound propagation in sound-absorbent ducts with superimposed air streams. *Technical Documentary Rep. No.* AMRL-TDR-62-140 (IV), University of Goettingen, FRG.

MICHALKE, A. 1965 On spatially growing disturbances in an inviscid shear layer. *J. Fluid Mech.* **23**, 521–544.

MUELLER, T. J. 1985 Low Reynolds number vehicles. *AGARD*-AG-288.

MUELLER, T. J. & BATILL, S. M. 1982 Experimental studies of separation of a two-dimensional airfoil at low Reynolds numbers. *AIAA J.* **20**, 457–463.

NISHIOKA, M. & MORKOVIN, M. V. 1985 Boundary layer receptivity to unsteady pressure gradients: experiments and overview. *J. Fluid Mech.* **171**, 219–261.

PARKER, R. 1966 Resonance effects in wake shedding from parallel plates: some experimental observations. *J. Sound Vib.* **4**, 62–72.

PFENNINGER, W. 1977 Laminar flow control: laminarization. *AGARD*-R-654, pp. 3.1–3.75.

ROSHKO, A. 1954 On the drag and shedding frequency of two-dimensional bluff bodies. *NACA Tech. Note* 3169.

RUMSEY, C. L. 1987 A computational analysis of flow separation over five different airfoil geometries at high angles-of-attack. *AIAA Paper No.* 87-0188.

SCHLICHTING, H. 1979 *Boundary Layer Theory*. McGraw-Hill.

SROKOWSKI, A. J. & ORSZAG, S. A. 1977 Mass flow requirements for LFC wing design. *AIAA Paper No.* 77-1222.

TAM, C. K. W. 1978 Excitation of instability waves in a two-dimensional shear layer by sound. *J. Fluid Mech.* **89**, 357–371.

ZAMAN, K. B. M. Q. & HUSSAIN, A. K. M. F. 1981 Turbulence suppression in free shear flow by controlled excitation. *J. Fluid Mech.* **103**, 133–160.